Modeling of Multiple Access Interference and BER Derivation for TH and DS UWB Multiple Access Systems

S. Niranjayan, *Student Member, IEEE*, A. Nallanathan, *Senior Member, IEEE*, and B. Kannan, *Member, IEEE*

***Abstract*— A novel analytical method is introduced for exact statistical modeling of multiple access interference (MAI), in time hopping pulse position modulation and pulse amplitude modulation (TH-PPM and TH-PAM) ultra wideband (UWB) systems operating in additive white Gaussian noise (AWGN) channels. Based on this method, exact bit error rates (BER) are expressed in simple formulas. In a similar fashion, the exact BER of direct sequence (DS) UWB is also derived for PAM modulation. The proposed modeling of MAI considers complete asynchronism in user access, and is also suitable for accurately modeling the MAI components contributed by individual paths in channels with Poisson arrivals, based on the time variables. We further extend this method to derive general expressions for the BER performance in log-normal fading multi-path channels. In the course of these derivations, we also introduce a more accurate numerical approach to evaluate the characteristic function (CF) of a lognormal random variable.**

***Index Terms*— Multiple access interference (MAI), performance evaluation, UWB.**

I. Introduction

RECENTLY, Ultra wideband (UWB) technology has attracted the research community as well as the industry due to its promising advantages in high speed, low power and short range wireless communication applications. Its extremely larger bandwidth provides high multiple access capability and robustness to multi-path conditions.

Theoretical tools for evaluating the performance in terms of bit error rate are important in simplifying the system design and deployment tasks. In the recent past, such theoretical evaluations of the BER of various UWB systems have been reported under different conditions.

Single user in AWGN channel was considered in [1] and [2]. Under these conditions, the problem is straight forward and the BER can be represented by the Q-function (or the Gaussian tail probability function) exactly. Single user in multi-path fading channel case was handled in [3] - [7]; and the problem was some what analytically tractable even for *Rake* receivers due to the absence of MAI.

System performance in AWGN channels considering multiple access interference (MAI) was addressed in [2], [8] - [10], where the MAI is modeled as a Gaussian random variable (Gaussian Approximation (GA)). With the GA assumption, the problem was simplified and became tractable with a simple closed form solution. In multi-user multi-path fading conditions, either the GA was used in deriving the average BER [2], [11] or the performance evaluation was based entirely on Monte-Carlo simulations [12].

The GA was proven as highly over-estimating the performance of TH systems [13] - [15]. As explained in [14], the failure of GA is due to the non-smooth nature of interference probability density function (PDF) and its concentration at some special values.

For multi-user AWGN channel, some non-GA alternative methods were proposed or used in [14] - [19]. In [14], analysis is performed for a synchronous TH-UWB and an approximated PDF of the interference was used for asynchronous case. An approach assuming rectangular monopulses has been presented in [15] and [19] for two different modulation schemes. A semi analytical method was introduced in [18], which uses the Gaussian quadrature rule (GQR) to perform the integration on the conditional BER to obtain the average BER. In [17], another approach is introduced using an approximate characteristic function for a fully asynchronous system. Another characteristic function based approach was introduced in [16] with more accurate modeling of MAI but with a quasi-synchronous channel.

The derivations in [14], [15], [17] - [19] are either approximate or pulse shape dependant or semi analytical and hence do not exactly model the MAI for an arbitrary pulse shape. Therefore a need arises to find an appropriate analytical model for the MAI in a fully asynchronous channel, independent of the pulse shape.

Also in [14], [15] and [19], it is assumed that the interferences caused by individual pulses residing in different frames are independent, and thus the total interference over one symbol duration was defined as a sum of number of independent and identically distributed (i.i.d.) random variables. But in reality, there exists a certain dependency among these variables; therefore the sum of the interferences from all the frames should be modeled directly from the basic principles without the i.i.d. assumption at the beginning. In

Manuscript received August 3, 2004; revised June 27, 2005; accepted November 7, 2005. The editor coordinating the review of this paper and approving it for publication is X. Shen.

S. Niranjayan is with the Department of Electrical and Computer Engineering, University of Alberta, Edmonton, Alberta T6G 2V4 Canada (e-mail: niranjan@icoremail.ee.ualberta.ca).

A. Nallanathan is with the Department of Electrical and Computer Engineering, National University of Singapore, 10, Kent Ridge Crescent, Block E4, Singapore, 119260 (e-mail: elena@nus.edu.sg).

B. Kannan is with the School of Electrical Engineering and Telecommunications, University of New South Wales, New South Wales, Australia (e-mail: kannanb@i2r.a-star.edu.sg).

Digital Object Identifier 10.1109/TWC.2006.04530.

[20], we performed the exact BER analysis for orthogonal TH-PPM UWB under full asynchronous access condition and by modeling the interference directly from basic principles.

In this paper, we present an exact and more realistic method to model the statistics of MAI for TH-PPM, TH-PAM and DS-PAM schemes in AWGN channel, considering full asynchronous access and the inter dependency of interferences from different frames. Using this model, the CF of the total interference is derived and the exact performance is expressed in closed forms in AWGN channels. Extensions of these derivations for TH-OOK (On-Off Keying), DS-PPM and DS-OOK are straight forward.

Furthermore, the performance of a single correlator receiver in multi-path channel is also derived using a simplified channel model. In the course of these derivations, an accurate numerical approach is also proposed to evaluate the characteristic function of a lognormal random variable for practical purposes. Finally the analytical BER performance results are compared with the Monte-Carlo simulation results to ensure the accuracy of the derivations.

The rest of this paper is organized as follows. A brief description of system models is presented in Section II. In Section III, accurate statistical models of the MAI in AWGN channel are presented. In Section IV, the characteristic functions of the MAI and the BER equations are derived. In Section V, fading channel case is addressed. Some numerical results are presented in Section VI. Finally, conclusions are given in Section VII.

II. System Models

A. Signal Model

The following notations are defined in common for all the three schemes considered. N_s represents the repetition code length or the total number of pulses in a bit period, T_f represents the frame length in TH systems, $D_j^u \in \{0,1\}$ is a random variable denoting the j^{th} transmitted binary data of user u, and $w(t)$ defines the waveform that a mono-pulse can assume. Further, T_c represents the hopping step size within a frame in TH-PPM/PAM systems or the chip length in DS systems, $c_i^u \in \{0,1,.....N_h-1\}$ represents the value of the random chip code of the u^{th} user in the i^{th} frame and δ denotes the modulation index (in PPM only). In a DS-PAM system $a_i^u \in \{\pm 1\}$ represents the signature sequence assigned to user u. The transmitted signal of the u^{th} user is represented by $v^u(t)$. For TH-PPM, TH-PAM and DS-PAM systems, $v^u(t)$ can be written as:

$$v^u(t)_{PPM} = \sqrt{E}\sum_{i=0}^{\infty} w\left[t - iT_f - c_i^u T_c - \delta D^u_{\lfloor i/Ns \rfloor}\right] \quad (1)$$

$$v^u(t)_{PAM} = \sqrt{E}\sum_{i=0}^{\infty} (-1)^{D^u_{\lfloor i/Ns \rfloor}} w\left[t - iT_f - c_i^u T_c\right] \quad (2)$$

$$v^u(t)_{DS-PAM} = \sqrt{E}\sum_{i=0}^{\infty} (-1)^{D^u_{\lfloor i/Ns \rfloor}} a_i^u w\left[t - iT_c\right] \quad (3)$$

respectively. Here, $D^u_{\lfloor i/Ns \rfloor}$ represents the data bit over the i^{th} frame, $\lfloor\ \rfloor$- represents the flooring operator. The energy of a mono-pulse is E and $w(t)$ is normalized such that, $\int_{-\infty}^{\infty} w(t)^2 dt = 1$.

A generalized UWB channel model can be expressed by the discrete channel impulse response

$$h^u(t) = \sum_{l=0}^{L-1} h_l^u \delta(t - \tau_l^u) \quad (4)$$

where h_l^u is the channel gain and τ_l^u is the total delay of the l^{th} signal path of user u. Therefore the received signal is given by $r(t) = \sum_{u=0}^{Nu-1}\sum_{l=0}^{L-1} h_l^u v^u(t - \tau_l^u) + n(t)$, where L is the number of significant energy paths, determination of which is based on the channel model adopted. $n(t)$ represents the additive white Gaussian noise (AWGN) signal.

The correlating template waveform $b_T(t)$ used for the detection of the j^{th} bit of the u^{th} user is defined as follows:

$$b_T(t)_{PPM} = \sum_{i=jN_s}^{(j+1)N_s-1} b_{PPM}\left(t - iT_f - c_i^u T_c\right) \quad (5)$$

$$b_T(t)_{PAM} = \sum_{i=jN_s}^{(j+1)N_s-1} w\left(t - iT_f - c_i^u T_c\right) \quad (6)$$

$$b_T(t)_{DS-PAM} = \sum_{i=jN_s}^{(j+1)Ns-1} a_i^u w\left[t - iT_c\right]. \quad (7)$$

where $b_{PPM}(t) = w(t) - w(t-\delta)$. The decision variable at the output of the correlator detector, which extracts the energy from the first path, is given by

$$r = \int_{jT_b}^{(j+1)T_b} sgn\left(h_0^u\right) \times b_T(t - \tau_0^u)\, r(t)\, dt = s + I + n \quad (8)$$

where T_b is the symbol period (is equal to N_sT_f in TH systems and N_sT_c in DS system), n is the filtered noise and s is the desired signal component given by $\left(h_o^u\right)^2 (-1)^{D_j^u} N_s\sqrt{E}\int_{-\infty}^{\infty} w(t) b_{PPM}(t)\, dt$ for PPM and $\left(h_o^u\right)^2 (-1)^{D_j^u} N_s\sqrt{E}$ for PAM modulation and $sgn(.)$ is the signum function. The MAI components (I) are given by (9) - (11).

Finally, the decision rule used by the detector is $D_j = 0 \Leftrightarrow r > 0$ *or* $D_j = 1 \Leftrightarrow r < 0$.

B. The Channel Model

The channel model in [21] was accepted by the standardization group, IEEE 802.15.3a, as the model for the evaluation of the proposals for UWB standardization activities [22], which accurately models a real UWB channel. This model contains multiple clusters (of rays) with random cluster-starting times, hence the power decaying profile (PDP) is segmented. Furthermore, the channel gain is modeled as a log-normal random variable with another lognormal variable acting on it to represent the shadowing effect. Therefore, it is a formidable task to develop accurate methods to find the BER performance using it. Therefore, in order to make the analysis theoretically tractable, certain simplifying assumptions are made in this paper. We define the channel gain h_l^u as a double sided lognormal variable, i.e., $20\log_{10}\left(|h_l^u|\right) \sim N\left(\mu_l^u, \sigma_l^u\right)$, where N represents the normal distribution. The PDP is defined by

$$I_{PPM} = \int_{jT_b}^{(j+1)T_b} h_o^u b_T(t-\tau_0^u)_{PPM} \sum_{u=0}^{N_u-1} \sum_{\substack{l=0 \\ l=1\, if\, u=0}}^{L-1} h_l^u v^u(t-\tau_l^u)_{PPM}\, dt \tag{9}$$

$$I_{PAM} = \int_{jT_b}^{(j+1)T_b} h_o^u b_T(t-\tau_0^u)_{PAM} \sum_{u=0}^{N_u-1} \sum_{\substack{l=0 \\ l=1\, if\, u=0}}^{L-1} h_l^u v^u(t-\tau_l^u)_{PAM}\, dt \tag{10}$$

$$I_{DS-PAM} = \int_{jT_b}^{(j+1)T_b} h_o^u b_T(t-\tau_0^u)_{DS-PAM} \sum_{u=0}^{N_u-1} \sum_{\substack{l=0 \\ l=1\, if\, u=0}}^{L-1} h_l^u v^u(t-\tau_l^u)_{DS-PAM}\, dt \tag{11}$$

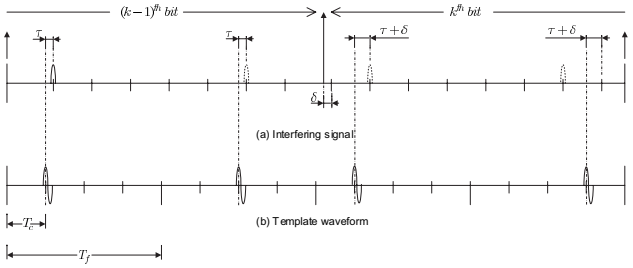

Fig. 1. An interfering signal (a) compared against the template wave form (b) of the desired user with $N_s = 4$ and $T_c = T_f/4$ for TH-PPM. Shown example is for $D_{k-1}D_k$=01.

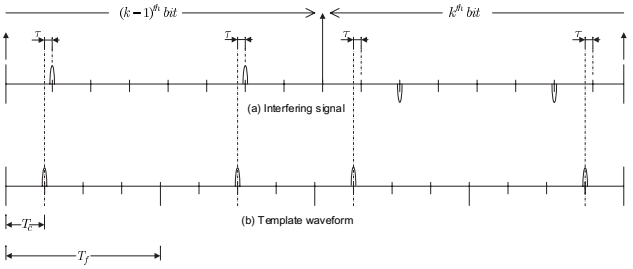

Fig. 2. An interfering signal (a) compared against the template wave form (b) of the desired user with $N_s = 4$ and $T_c = T_f/4$ for TH-PAM.

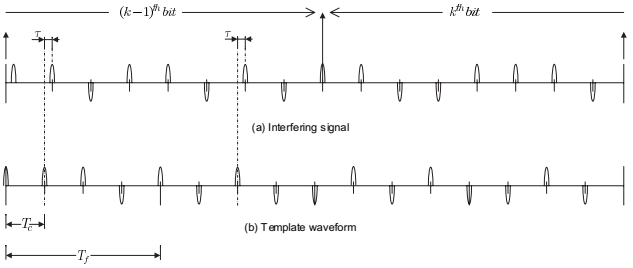

Fig. 3. An interfering signal (a) compared against the template wave form (b) of the desired user with$N_s = 8$ for DS- PAM.

a simple decaying exponential function and it can be simply expressed in terms of the path number l as $E\left\{(h_l^u)^2\right\} = e^{-\rho l}$, where ρ is the decay factor. Finally the arrival times are assumed fixed and evenly spaced. However, the derivations presented later are also valid for the case where the arrival times are unevenly spaced. A similar simplified model can be found in [3].

III. Multiple Access Interference Model for AWGN Channel

The impulse wave $w(t)$ can be any narrow pulse waveform satisfying the spectral requirements. The autocorrelation function of $w(t)$ and the cross correlation function $R_{wb}(\tau)$ are respectively defined as $R_{ww}(\tau) = \int_{-\infty}^{\infty} w(t)w(t-\tau)dt$ and $R_{wb}(\tau) = \int_{-\infty}^{\infty} w(t)b(t-\tau)dt$, where $b(t)$ represents a template pulse (In PPM, template pulse refers to one of the N_s bi-pulse waveforms of $b_T(t)_{PPM}$ and in PAM it refers to a mono-pulse). $R_{wb}(\tau)$is equivalent to $R_{ww}(\tau) - R_{ww}(\tau+\delta)$ for PPM modulation and to $R_{ww}(\tau)$for PAM modulation. If τ_m is the impulse width of $w(t)$, both $R_{ww}(\tau)$ and $R_{wb}(\tau)$ will be confined within the ranges $[-\tau_m, \tau_m]$ and $[-(\tau_m+\delta), \tau_m]$ respectively.

The first step in modeling the total MAI is the modeling of the interference contributed by one template pulse when correlated against the interfering signal, arriving through a single path of an interfering user. This interference related to one template pulse can be modeled by the function $R_{wb}(\tau)$ by attributing the randomness to a proper random variable τ.

A. Modeling of τ

In Fig. 1, Fig. 2 and Fig. 3 the small 'ticks' denote the pulse origins, where pulse origins are defined as the points in the time axis that can possibly accommodate a mono-pulse. The interfering signal's time axis consists of an infinite sequence of pulse origins. In calculating the interference generated by a template pulse, we are only interested in its closest interfering mono-pulses since the pulses falling far apart will have zero correlation with the template pulse of interest. It is reasonable to assume that a maximum of one mono-pulse from the interferer collides with a template pulse at a given time. We define a variable τ as the time difference from the first template pulse to its *closest* pulse origin of the interfering signal (Fig. 1, 2 & 3). In TH systems, with the assumption of a random chip code, the closest pulse origin may have a mono-pulse with a probability equal to $1/N_h$, where N_h being the number of chips in a frame. But in DS systems every pulse origin is guaranteed to have a mono-pulse.

Since τ is the distance to the neighboring pulse origin, the

maximum value of $|\tau|$ is equal to $T_c/2$. Therefore the range of τ is given by, $\tau \in [-T_c/2,\ T_c/2]$. In an AWGN channel the absolute positioning of pulse origins in the interfering signal's time axis is determined by the asynchronous time delay α^u, T_c, δ and D_j^u. But, since T_c and δ are necessarily much smaller than the range of the uniform random variable α_u, the effect due to the discreteness in the distributions of the chip code and the data bit will be eliminated. Hence, the distribution of τ will eventually become *uniform within the above range* (It should be noted that this uniformity is not an assumption, it is an exact scenario unless someone chose inappropriately smaller values for N_s, like 1 or 2).

In a channel with delays related to Poisson arrivals, the maximum delay spread will be much smaller than N_sT_f (to avoid ISI, T_f is usually set larger than the maximum delay spread). Therefore the distribution of τ will be approximately uniform even in a multi-path channel. This is verified with simulations. The results are simple and obvious, therefore not presented here considering space limitation.

According to the definition of $v^u(t)$, it is assumed that there is no extra guard time provided between adjacent bits, except the inherent clearance available due to the chip time T_c. As in [17], [18], we also assume that T_f is spanned by an integer number of chip durations, i.e., $T_c = T_f/N_h$ in TH systems.

B. TH-PPM System

Fig. 1 depicts one interfering signal against the template wave form of the desired user, throughout a full bit duration for TH-PPM. It should be noted that a maximum of one bit changeover can occur during the considered time window (the interfering signal changes from $(k-1)^{th}$ bit to k^{th} bit). An arbitrary chip pattern is assumed for user 0. The interfering signal is viewed as an infinite sequence of mono-pulses. Its time axis consists of two sets of pulse origins (as marked in the diagram) corresponding to $(k-1)^{th}$ and k^{th} bit durations and the elements within each set are equally spaced.

Since we defined τ as the distance to the closest interfering pulse origin from the first template pulse, the interference related to the first template pulse is $R_{wb}(\tau)$ with a probability of occurrence $1/N_h$. It can be noted that all pulse origins in the $(k-1)^{th}$ bit are shifted by τ, relative to their adjacent chip positions in the template signal. From these points, we arrive at the following conclusions: Any pulse of the interferer within the $(k-1)^{th}$ bit duration can contribute to a correlation equal to $R_{wb}(\tau)$, with the probability $(1/N_h)$. Within the k^{th} bit's region, all the pulse origins can have an additional shift equal to $\delta, 0$ or $-\delta$; depending on the dibit $D_{k-1}D_k$. In this region the distance from a template pulse to it's closest interfering pulse can take following 3 different values; τ when $D_{k-1}D_k$ is 00 or 11 , μ^+ when $D_{k-1}D_k$ is 01 and μ^- when $D_{k-1}D_k$ is 10, where

$$\mu^+ = \begin{cases} \tau+\delta & ;\ if\ \tau+\delta \le \frac{T_c}{2} \\ \tau+\delta-T_c & ;\ if\ \tau+\delta \ge \frac{T_c}{2} \end{cases}$$
$$\mu^- = \begin{cases} \tau-\delta & ;\ if\ \tau-\delta \ge -\frac{T_c}{2} \\ T_c+\tau-\delta & ;\ if\ \tau-\delta \le -\frac{T_c}{2} \end{cases} \quad , \qquad (12)$$

(Note that we assume $\delta < T_c$). And the corresponding interference term is $R_{wb}(\tau)$ or $R_{wb}(\mu^+)$ or $R_{wb}(\mu^-)$. One can infer from the above derivations that for a given τ, the total interference from the interfering signal can only assume the values defined in (13), where n_1 and n_2 are positive integers with $n_1+n_2 \le N_s$ representing the resulting number of collisions in $(k-1)^{th}$ and k^{th} bit durations, respectively. This clearly shows that the interferences caused by individual pulses in different frames are not purely independent which contradicts with the assumptions in [14], [15] and [19]. By evaluating the corresponding probabilities of the discrete values of $I^u_{PPM/\tau}$ and using the distribution of τ, the statistical modeling of I^u_{PPM} is complete.

With respect to the possible values of $I^u_{PPM/\tau}$ given by (13), we define a set of probabilities in (14) - (16) as shown at the top of the next page.

It can be shown that $P_{01}(n_1,n_2) = P_{10}(n_1,n_2) = P(n_1,n_2)$ (refer to Appendix I for the derivations).

C. TH-PAM System

Fig. 2 shows an interfering signal against the correlating template waveform for PAM. According to the model described in section II, the interference related to the first template pulse is $\pm R_{ww}(\tau)$, where the sign depends on the $(k-1)^{th}$ data bit, and the probability of this occurrence is $1/N_h$. Similarly all the template pulses (note that now the template pulse is a single mono-pulse) in the k^{th} bit duration can generate a correlation $\pm R_{ww}(\tau)$, with the probability of $1/N_h$, and the sign is determined by the k^{th} bit.

Therefore, the total interference over the bit duration becomes $I^u_{PAM/\tau} = n_1R_{ww}(\tau)$, where, $n_1 \in \{-N_s, -(N_s-1), ..., N_s\}$. The probability $P\left(I^u_{PAM/\tau} = n_1R_{ww}(\tau)\right)$ is defined as $P_{PAM}(n_1)$, where $P_{PAM}(n_1) = P_{PAM}(-n_1) = P_{00}(n_1) + P_{01}(n_1) + P_{10}(n_1) + P_{11}(n_1)$ for $n_1 \in \{-N_s, ..., N_s\}$ (refer to Appendix II for the proofs).

D. DS-PAM System

Fig. 3 shows a typical interfering condition of DS-PAM signals. Since the factor $(-1)^{D^u_{\lfloor i/N_s \rfloor}}$ and the chip code a^u_i are independent and both jointly modify the pulse polarity with equal probability, the resulting coefficient $(-1)^{D^u_{\lfloor i/N_s \rfloor}} \times a^u_i$ can be modeled by another equiprobable bipolar random variable. Therefore, with the assumption of a long code, the need for considering the bit changeover is eliminated. Each template pulse will generate an interference component $\pm R_{ww}(\tau)$ with equal probability and hence, the possible values of the total interference conditioned on τ is given by $I^u_{DS-PAM/\tau} = n_1R_{ww}(\tau)$, where $n_1 \in \{-N_s,\ -N_s+2, ...N_s-2,\ N_s\}$. The conditional probability $P_{DS}(n_1)$ is defined as $P_{DS}(n_1) = P\left(I^u_{DS-PAM/\tau} = n_1R_{ww}(\tau)\right)$ and it is straight forward to show, using binomial distribution theory, that $P_{DS}(n_1) = C^{N_s}_{\frac{(N_s+|n_1|)}{2}}(1/2)^{N_s}$ for $n_1 \in \{-N_s,\ -N_s+2, ...,\ N_s\}$.

IV. Derivation of CF and BER for AWGN Channel

A. TH-PPM

Considering an AWGN channel, the total MAI component I_{PPM} is now given by, $I_{PPM} = \sum_{u=1}^{N_u-1} I^u_{PPM}$. By

$$I^u_{PPM/\tau} = \left[n_1 R_{wb}(\tau) + n_2 R_{wb}(\mu^+)\right] \quad or \quad \left[n_1 R_{wb}(\tau) + n_2 R_{wb}(\mu^-)\right] \tag{13}$$

$$P_{01}(n_1, n_2) = P\left(\left\{I^u_{PPM/\tau} = n_1 \times R_{wb}(\tau) + n_2 \times R_{wb}(\mu^+)\right\} \quad and \quad \{D_{k-1}D_k = 01\}\right), \tag{14}$$

$$P_{10}(n_1, n_2) = P\left(\left\{I^u_{PPM/\tau} = n_1 \times R_{wb}(\tau) + n_2 \times R_{wb}(\mu^-)\right\} \quad and \quad \{D_{k-1}D_k = 10\}\right), \tag{15}$$

$$P(n_1) = P\left(\left\{I^u_{PPM/\tau} = n_1 \times R_{wb}(\tau)\right\} \quad and \quad \{D_{k-1}D_k = 00\, or\, 11\}\right). \tag{16}$$

$$\begin{aligned}\Phi_{(I^u_{PPM/\tau})} &= \sum_{n_1=0}^{Ns}\sum_{n_2=0}^{Ns-n_1} P(n_1, n_2)\left[\exp\left(jw\left(n_1 R_{wb}(\tau) + n_2 R_{wb}(\mu^+)\right)\right) + \exp\left(jw\left(n_1 R_{wb}(\tau) + n_2 R_{wb}(\mu^-)\right)\right)\right] \\ &\quad + \sum_{n_1=0}^{Ns} P(n_1)\left[\exp\left(jwn_1 R_{wb}(\tau)\right)\right]\end{aligned} \tag{18}$$

$$\begin{aligned}\Phi' &= \sum_{n_1=0}^{Ns}\sum_{n_2=0}^{Ns-n_1} P(n_1, n_2)\left[\cos\left[w\left(n_1 R_{wb}(\tau) + n_2 R_{wb}(\mu^+)\right)\right] + \cos\left[w\left(n_1 R_{wb}(\tau) + n_2 R_{wb}(\mu^-)\right)\right]\right] \\ &\quad + \sum_{n_1=0}^{Ns} P(n_1)\cos\left[n_1 R_{wb}(\tau)\right]\end{aligned} \tag{21}$$

definition, the CF of I_{PPM} is given by $\Phi_{I_{PPM}}(w) = E\{\exp(jwI_{PPM})\}$. The CF, $\Phi_{(I^u_{PPM})}(w)$ can be expressed as

$$\Phi_{(I^u_{PPM})}(w) = \frac{1}{T_c}\int_{\frac{-T_c}{2}}^{\frac{T_c}{2}} \Phi_{(I^u_{PPM/\tau})} d\tau, \tag{17}$$

where the conditional CF $\Phi_{(I^u_{PPM/\tau})}$ is given by (18).

Generally, the pulse waveform $w(t)$ assumes a symmetric shape; therefore the distribution of I^u_{PPM} also becomes symmetric. Hence, we can write

$$\begin{aligned}&\Phi_{(I^u_{PPM})}(w) = \Phi_{(-I^u_{PPM})}(w) \\ =\ &\frac{1}{2}\left(\Phi_{(I^u_{PPM})}(w) + \Phi_{(-I^u_{PPM})}(w)\right).\end{aligned} \tag{19}$$

Using (19), we can get rid of the complex integration in (17) and obtain the following real valued expression:

$$\Phi_{(I^u_{PPM})}(w) = \frac{1}{T_c}\int_{\frac{-T_c}{2}}^{\frac{T_c}{2}} \Phi' d\tau \tag{20}$$

where Φ' is given by (21).

Since I^u_{PPM} are assumed i.i.d, $\Phi_{I_{PPM}}(w)$ is given by $\Phi_{I_{PPM}}(w) = \left[\Phi_{I^u_{PPM}}(w)\right]^{N_u - 1}$. The CF of the AWGN component n_{PPM} is given by $\Phi_{n_{PPM}}(w) = \exp\left(\frac{-w^2 N_o R_{wb}(0) N_s}{2}\right)$, where $N_o/2$ is the double sided power spectral density of the noise.

Now the bit error probability of the binary modulation scheme is given by

$$\begin{aligned}P_e &= \tfrac{1}{2}P(r \geq 0/D_j = 1) + \tfrac{1}{2}P(r \leq 0/D_j = 0) \\ &= P(r \leq 0/D_j = 0) \\ &= P(I_{PPM} + n_{ppm} \leq -N_s\sqrt{E}R_{wb}(0)/D_j = 0).\end{aligned} \tag{22}$$

With the help of few Fourier transform manipulations, P_e can be expressed as follows,

$$\begin{aligned}P_e = \frac{1}{2} - \frac{1}{2\pi}\int_{-\infty}^{\infty} &\frac{\Phi_{I_{PPM}}(-w)}{jw}\Phi_{n_{PPM}}(w) \\ &\times \exp\left(jw\sqrt{E}N_s R_{wb}(0)\right) dw.\end{aligned} \tag{23}$$

Since $\Phi_{I_{PPM}}(w)$ and $\Phi_{n_{PPM}}(w)$ are real and even-symmetric, the integral in equation (23) reduces to a convenient real function, which is given by

$$\begin{aligned}P_e = \frac{1}{2} - \frac{\sqrt{E}N_s R_{wb}(0)}{\pi}\int_0^{\infty} &\Phi_{I_{PPM}}(w)\Phi_{n_{PPM}}(w) \\ &\times \text{sinc}\left(\frac{\sqrt{E}N_s R_{wb}(0) w}{\pi}\right) dw.\end{aligned} \tag{24}$$

With the substitutions $w_o = \sqrt{E}w$ and $\gamma = \frac{N_s E}{N_o}$, equation (24) takes an alternative form

$$\begin{aligned}P_e = \frac{1}{2} - \frac{N_s R_{wb}(0)}{\pi}\int_0^{\infty} &\Phi_{\bar{I}_{PPM}}(w_o)\exp\left(\frac{-w_o^2 N_s^2 R_{wb}(0)}{2\gamma}\right) \\ &\times \text{sinc}\left(\frac{N_s R_{wb}(0) w_o}{\pi}\right) dw_o\end{aligned} \tag{25}$$

where $\Phi_{\bar{I}_{PPM}}(w_o) = E\left\{\exp\left[jw_o\left(\frac{I_{PPM}}{\sqrt{E}}\right)\right]\right\}$ is the CF of the normalized interference.

B. TH-PAM

Similarly, the CF of the total interference is given by $\Phi_{I_{PAM}}(w) = \left[\Phi_{I^u_{PAM}}(w)\right]^{N_u - 1}$, where

$$\Phi_{(I^u_{PAM})}(w) = \frac{1}{T_c}\int_{-\tau_m}^{\tau_m} \Phi_{(I^u_{PAM/\tau})} d\tau + P_o. \tag{26}$$

The conditional CF $\Phi_{(I^u_{PAM/\tau})}$ is given by $\Phi_{(I^u_{PAM/\tau})} = P_{PAM}(0) + 2\sum_{1}^{Ns} P_{PAM}(n_1) \times \cos(w n_1 R_{ww}(\tau))$. The constant term P_o in (26) represents the probability that τ falls within $\left[-\frac{T_c}{2}, -\tau_m\right] \cup \left[\tau_m,\ \frac{T_c}{2}\right]$, i.e., the probability that $R_{ww}(\tau)$ is strictly zero within $\left[-\frac{T_c}{2},\ \frac{T_c}{2}\right]$. Therefore, $P_0 = 1 - \frac{2\tau_m}{T_c}$ (where the condition $2\tau_m \leq T_c$ is clearly understood in UWB signal design). In analogy with (22) we can obtain the following probability of error for a PAM system

$$P_e = P(I_{PAM} + n_{PAM} \leq -N_s\sqrt{E}R_{ww}(0)/D_j = 0). \quad (27)$$

It can be shown that $\Phi_{n_{PAM}}(w) = \exp\left(\frac{-w_o^2 N_s^2 R_{ww}(0)}{4\gamma}\right)$. Using the symmetry of I_{PAM}, the BER of a binary PAM system is given by

$$P_e = \frac{1}{2} - \frac{N_s R_{ww}(0)}{\pi} \int_0^\infty \Phi_{\bar{I}_{PAM}}(w_o)\ \exp\left(\frac{-w_o^2 N_s^2 R_{ww}(0)}{4\gamma}\right) \times \text{sinc}\left(\frac{N_s R_{ww}(0) w_o}{\pi}\right) dw_o. \quad (28)$$

C. DS-PAM

The CF of single user interference in DS-PAM systems is given by

$$\Phi_{(I^u_{DS-PAM})} = \frac{1}{T_c}\int_{-\tau_m}^{\tau_m} \sum_{n_1 \in \{-N_s, -N_s+2, \ldots, N_s\}} P_{DS}(n_1) \times \exp(jw n_1 R_{ww}(\tau))\, d\tau + P_o \quad (29)$$

where $P_o = 1 - \frac{2\tau_m}{T_c}$ is the probability that τ falls within the range $\left[-\frac{T_c}{2}, -\tau_m\right] \cup \left[\tau_m,\ \frac{T_c}{2}\right]$ i.e., the probability that $I^u_{DS-PAM/\tau}$ is strictly zero. Equation (29) can be reduced to a real function form by using the symmetry of n_1, hence we obtain

$$\Phi_{(I^u_{DS-PAM})} = \frac{2}{T_c}\int_{-\tau_m}^{\tau_m} P_{DS}(0) + \sum_{n_1 \in \{N_s, N_s-2, \ldots, 2\ or\ 1\}} P_{DS}(n_1) \times \cos(w n_1 R_{ww}(\tau))\ d\tau + P_o. \quad (30)$$

It should be noted that the lower limit of the summation is either 2 or 1 since N_s can be even or odd and $P_{DS}(0) = 0$ if N_s is odd. Finally the average bit error probability for DS-PAM systems is given by

$$P_e = \frac{1}{2} - \frac{N_s R_{ww}(0)}{\pi} \times \int_0^\infty \Phi_{\bar{I}_{DS-PAM}}(w_o)\ \exp\left(\frac{-w_o^2 N_s^2 R_{ww}(0)}{4\gamma}\right) \times \text{sinc}\left(\frac{N_s R_{ww}(0) w_o}{\pi}\right) dw_o. \quad (31)$$

V. Performance under Fading Channels

In the previous sections, we derived the CF of the total interference, I^u accurately for TH-PPM (I^u_{PPM}), TH-PAM (I^u_{PAM}) and DS-PAM (I^u_{DS-PAM}) modulations under AWGN channel conditions. In fading multi-path channels, the basic element in modeling the multiple access interference is I^u_l, the interference caused by the l^{th} arrival path from the u^{th} user.

The total inteference, I^u_l can be modeled as a product of two random variables (R.V), i.e., $I^u_l = h^u_l \times I(\tau)$, where $I(\tau)$ is a statistical equivalent to I^u, which is already defined for TH-PPM, TH-PAM and DS-PAM separately under the AWGN channel conditions. The notation τ has also been defined earlier. It should be noted that the path and user dependency of I^u_l is attributed to the gain parameter h^u_l and $I(\tau)$ is assumed to be independent of h^u_l. This independent assumption is reasonable since τ is defined as the distance to the closest chip position from the first template pulse, whereas the distribution of h^u_l is reliant on absolute path arrival times.

The CF of I^u_l conditioned on $I(\tau)$ is defined by $\Phi_{I^u_l/I(\tau)}(w) = E\left\{e^{jwI^u_l}/I(\tau)\right\}$. Therefore,

$$\Phi_{I^u_l}(w) = \int_{-\infty}^{\infty} \Phi_{I^u_l/I(\tau)}(w) \times P_{I(\tau)}(I)\, dI. \quad (32)$$

Since the statistics of $I(\tau)$ is already defined implicitly in sections III.B, III.C and III.D for TH-PPM, TH-PAM and DS-PAM, respectively, (32) is solvable accurately if a closed form solution for $\Phi_{I^u_l/I(\tau)}(w)$ is known.

The channel coefficient h^u_l has a double sided lognormal distribution according to the channel model stated in [21]. Therefore, for a given value of $I(\tau)$, I^u_l can be equivalently modeled by $p\,|I^u_l|$, where p represents equi-probable positive and negative polarities and has the distribution $P_p(p) = 0.5\,(\delta(p+1) + \delta(p-1))$. The distribution of $|I^u_l/I(\tau)|$ is also lognormal since it is generated by multiplying a lognormal variable by a constant term. Therefore,

$$\begin{aligned}\Phi_{I^u_l/I(\tau)}(w) &= \int_{-\infty}^{\infty} P_{I^u_l/I(\tau)}(I^u_l) e^{jwI^u_l} dI^u_l \\ &= \int_0^{\infty} P_{|I^u_l|/I(\tau)}\left(|I^u_l|\right) \cos\left(w\,|I^u_l|\right)\, d\,|I^u_l| \\ &= Re\left\{\Phi_{LN}(w, \sigma, \mu)\right\}.\end{aligned} \quad (33)$$

where, Φ_{LN} denotes the characteristic function of a log normal variable. The parameters σ and μ are given by $\sigma^2 = Var\left\{20\log_{10}\left(|I^u_l/I(\tau)|\right)\right\}$ and $\mu = E\left\{20\log_{10}\left(|I^u_l/I(\tau)|\right)\right\}$. But a simple closed form solution for the CF of a log normal variable is not known [23], [24]. A solution in the form of an infinite series is proposed in [25], but the evaluation of the series coefficients up to an order to achieve acceptable accuracy is much difficult. Therefore the CF should be estimated by suitable numerical methods. Gaussian Quadrature methods are preferable as the integral can be approximated in the form of a finite series. A Gauss-Hemite quadrature integral is used in [26], but when tested for few sets of values of σ, μ and w, we found that the method dose not work well over the possible ranges of values of the parameters. In some cases the estimation errors are very high. A more detailed analysis on the numerical evaluation of the CF is presented in [24] which also proposes a new method based on Cleanshaw-Curtis algorithm.

The particular problem we address here requires the estimation of the CF over a larger range of μ and σ is a constant for a channel and its typical values are around 3dB to 6dB. It was

found by our tests that a single approximation method is likely to fail over some sub-ranges of μ values. Therefore, in order to alleviate this, we introduce a multi-segmented approach.

The power of the l^{th} path can be related to the power of the first path, $E\left\{(h_0^u)^2\right\}$ by

$$E\left\{(h_l^u)^2\right\} = E\left\{(h_0^u)^2\right\} \times e^{-\rho l} \tag{34}$$

where $0 \le l \le (L-1)$ and ρ is the decay factor. We assume equally spaced paths in the theoretical model for convenience. The distribution of $|h_l^u|$ is given by

$$P_{|h_l^u|}(h) = \frac{20}{\ln(10)}\frac{1}{h}\frac{1}{\sqrt{2\pi}\sigma_1}\exp\left(\frac{-(20\log_{10}(h)-\mu_l^u)^2}{2\sigma_1^2}\right) \tag{35}$$

where σ_1 is the dB spread of the log normal fading i.e., ($\ln(.)$ is the natural logarithm), $\sigma_1^2 = E\left\{(20\log_{10}(h)-\mu_l^u)^2\right\}$ and μ_l^u can be written as

$$\mu_l^u = \mu_o^u - \frac{10}{\ln 10}\rho l. \tag{36}$$

Further, we assume that the parameters μ_l^u are independent of u. This assumption is quite valid in case of a centralized network with perfect power control, but it is deemed only to simplify the derivations otherwise. Therefore, all the gain variables $h_o^u, ..., h_{L-1}^u$ have equal dB spread σ_1 and μ_l^u according to (36).

A. A Multi-Segmented Numerical Approach for the Evaluation of CF

The function $Re\{\Phi_{LN}(w,\sigma,\mu)\}$ is to be approximated over the possible ranges of values of σ and μ, where σ remains constant for a particular channel. Parameter μ, which is given by the equation $\mu = \mu_l^u + 20\log_{10}(|I(\tau)|)$ spans over an infinite range $[-\infty,\ \mu_H]$, where $\mu_H = \mu_l^u + 20\log_{10}(|I(\tau)|_{\max})$ is a finite number. The value of μ_H is controllable by scaling the total energy of the received signal, if required. Using a dummy variable x, $Re\{\Phi_{LN}(w,\sigma,\mu)\}$ is expressed as

$$Re\{\Phi_{LN}(w,\sigma,\mu)\} = \int_0^\infty \frac{20}{\ln 10}\frac{1}{x}\frac{1}{\sqrt{2\pi}\sigma}\exp\left(\frac{-(20\log_{10}(x)-\mu)^2}{2\sigma^2}\right)\times\cos(wx)\,dx. \tag{37}$$

An alternative form of (37), with the substitution $y = 20\log_{10}(x)$ is given by

$$Re\{\Phi_{LN}(w,\sigma,\mu)\} = \int_{-\infty}^{\infty}\frac{1}{\sqrt{2\pi}\sigma}\exp\left(\frac{-(y-\mu)^2}{2\sigma^2}\right)\times\cos(w10^{(y/20)})\,dy. \tag{38}$$

By examining different Gaussian Quadrature methods, we found that Gauss-Laguerre method provides good approximation for fairly larger values of μ. Therefore, it is straight forward to show that

$$Re\{\Phi_{LN}(w,\sigma,\mu)\} = \sum_{k=1}^{N_p} W(x_k)e^{x_k}\frac{20}{\ln 10}\frac{1}{x_k}\frac{1}{\sqrt{2\pi}\sigma}\times\exp\left(\frac{-(20\log_{10}(x_k)-\mu)^2}{2\sigma^2}\right)\times\cos(wx_k) \tag{39}$$

where x_k is the k^{th} zero of the $N_p$order Laguerre polynomial $L_{N_P}(x)$, and the corresponding weights $W(x_k)$ are given by $W(x_k) = \frac{x_k}{(N_p+1)^2\left[L_{N_p+1}(x_k)\right]^2}$.

The integrand in (37) becomes a steeper function when μ grows smaller and because of this, the Gauss-Laguerre method becomes inaccurate even when N_p is set at a larger value (e.g. N_p= 32).

The alternative form (38) would help to resolve this problem since the integrand in this expression is a smooth function except the fast oscillating positive tail. For larger negative values of μ the integrand can be truncated effectively within the range $[\mu - 5\sigma,\ \mu + 5\sigma]$. The error in neglecting the tails is lower than $2Q(5)$ ($\simeq 5.7\times10^{-7}$), where Q denotes the Gaussian Q-function. Therefore the truncated integral of $Re\{\Phi_{LN}(w,\sigma,\mu)\}$can be expressed as

$$Re\{\Phi_{LN}(w,\sigma,\mu)\} \simeq \int_{\mu-5\sigma}^{\mu+5\sigma}\frac{1}{\sqrt{2\pi}\sigma}\exp\left(\frac{-(y-\mu)^2}{2\sigma^2}\right)\times\cos\left(w\,10^{(y/20)}\right)dy. \tag{40}$$

This can be effectively computed by Gauss-Legendre integration, which yields

$$Re\{\Phi_{LN}(w,\sigma,\mu)\} \simeq 5\sigma\sum_{k=1}^{N_p} W(y_k)\frac{1}{\sqrt{2\pi}\sigma}\exp\left(\frac{-25y_k^2}{2}\right)\times\cos\left(w\,10^{((5\sigma y_k+\mu)/20)}\right) \tag{41}$$

where y_k are the abscissas of the N_p^{th} order Legendre polynomial $G_{N_p}(y)$. The weight factors $W(y_k)$ are given by $W(y_k) = \frac{2}{\left(1-y_k^2\right)\left[G'_{N_p}(y_k)\right]^2}$.

Finally, by noting the fact that $\lim_{\mu\to-\infty}\left\{\frac{20}{\ln 10}\frac{1}{x}\frac{1}{\sqrt{2\pi}\sigma}\exp\left(\frac{-(20\log_{10}(x)-\mu)^2}{2\sigma^2}\right)\right\} = \delta(x)$, where $\delta(.)$ is the Dirac delta function, we approximate the PDF by a delta function for extremely smaller values of μ which actually represents the condition of near zero interference. Some numerical values are shown here to compare the accuracy of the method proposed. The function $Re\{\Phi_{LN}(w,\sigma,\mu)\}$ is evaluated at $w = 0$, $\sigma = 6$ and $\mu = -1.3$ using our method with $N_p = 10$ and the Gauss-Hermite method with $N_p = 30$, and the results obtained are 1.0001 and 0.7433, respectively. This shows that the proposed method achieves higher accuracy with less number of terms in the summation. As a second example, when evaluated at $w = 0$, $\sigma = 6$ and $\mu = -50$ with $N_p = 31$ for both methods, the results are 0.9725 and 7.19×10^{-13}, respectively. In another example, when evaluated at $w = 0.1$, $\sigma = 6$ and $\mu = -1.3$ with $N_p = 10$ for our method and $N_p = 30$ for the the Gauss-Hermite method, the results are 0.9908 and 0.5719 respectively, whereas the actual value obtained by the trapezoidal rule with high dense sampling is 0.9905.

B. CF of the Total Interference

It is straight forward to derive $\Phi_{I_l^u}(w)$ for all the UWB schemes considered in this paper, from (32). For TH-PPM we

get

$$\Phi_{I_l^u}(w) = \frac{1}{T_c} \int_{-\frac{T_c}{2}}^{\frac{T_c}{2}} \left(\sum_{n_1=0}^{Ns} \sum_{n_2=0}^{Ns-n_1} \left[Re\left\{\Phi_{LN}(w,\sigma_1,\mu_1)\right\} + Re\left\{\Phi_{LN}(w,\sigma_1,\mu_2)\right\} \right] P(n_1,n_2) + \sum_{n_1=0}^{Ns} Re\left\{\Phi_{LN}(w,\sigma_1,\mu_3)\right\} P(n_1) \right) d\tau \quad (42)$$

where

$$\mu_1 = \mu_l^u + 20\log_{10}\left(\left|\left(n_1 R_{wb}(\tau) + n_2 R_{wb}(\mu^+)\right)\right|\right), \quad (43)$$

$$\mu_2 = \mu_l^u + 20\log_{10}\left(\left|\left(n_1 R_{wb}(\tau) + n_2 R_{wb}(\mu^-)\right)\right|\right), \quad (44)$$

$$\mu_3 = \mu_l^u + 20\log_{10}\left(\left|n_1 R_{wb}(\tau)\right|\right). \quad (45)$$

For PAM, we get

$$\Phi_{I_l^u}(w) = \frac{1}{T_c} \int_{-\tau_m}^{\tau_m} \sum_{n_1=-N_s}^{N_s} Re\left\{\Phi_{LN}(w,\sigma_1,\mu_1)\right\} P_{PAM}(n_1)\, d\tau + P_o \quad (46)$$

where $\mu_1 = \mu_l^u + 20\log_{10}\left(\left|n_1 R_{ww}(\tau)\right|\right)$.
For DS-PAM, we get

$$\Phi_{I_l^u}(w) = \frac{1}{T_c} \int_{-\tau_m}^{\tau_m} \sum_{n_1 \in \{-N_s,-N_s+2,\ldots,N_s\}} Re\left\{\Phi_{LN}(w,\sigma_1,\mu_1)\right\} P_{DS}(n_1)\, d\tau + P_o \quad (47)$$

where $\mu_1 = \mu_l^u + 20\log_{10}\left(\left|n_1 R_{ww}(\tau)\right|\right)$.

It should be noted that once $\Phi_{I_o^u}$ is found, $\Phi_{I_l^u}$ can be estimated using the following relationship:

$$\Phi_{I_l^u}(w) = \Phi_{I_o^u}\left(we^{-\rho l/2}\right) for l \in \{1,2,.....L-1\} \quad (48)$$

To make our analysis tractable, we also assume that I_l^u are independent for $l \in \{0,1,2,.....L-1\}$, and as in the AWGN case, the total interference from each user is assumed identical and independent. Therefore the CF of I is given by, $\Phi_I(w) = \left[\prod_{l=0}^{L-1} \Phi_{I_o^u}\left(we^{-\rho l/2}\right)\right]^{Nu}$.

C. The BER Probabilities of a Correlator Receiver

Let us assume that the first path, which is most probably the largest, is extracted at the receiver for detection. The conditional BER of the system is given by:

For TH-PPM

$$P_{e_{/h_o^u}} = \frac{1}{2} - \frac{\sqrt{E}N_s R_{wb}(0)\left|h_o^u\right|}{\pi} \times \int_0^\infty \Phi_I(w)\, \exp\left(\frac{-Ew^2 N_s^2 R_{wb}(0)}{2\gamma}\right) \times \mathrm{sinc}\left(\frac{\sqrt{E}N_s R_{wb}(0)\left|h_o^u\right| w}{\pi}\right) dw. \quad (49)$$

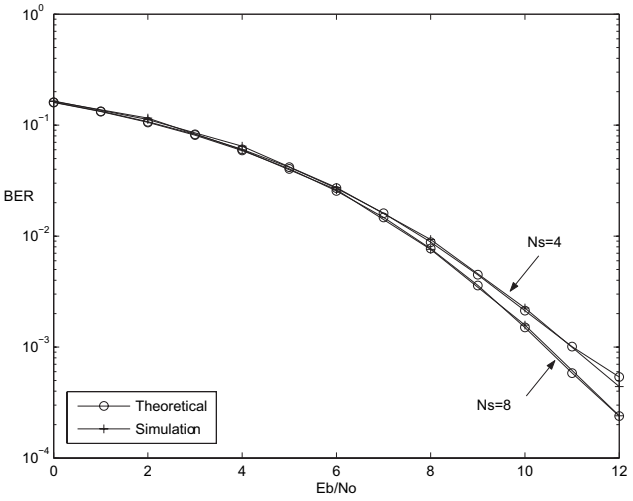

Fig. 4. Theoretical and simulation performance of TH-PPM compared for $N_s = 4$ and $N_s = 8$, with $T_c = 8ns$ and $\delta = 1.5ns$.

For TH- PAM and DS-PAM

$$P_{e_{/h_o^u}} = \frac{1}{2} - \frac{\sqrt{E}N_s R_{ww}(0)\left|h_o^u\right|}{\pi} \times \int_0^\infty \Phi_I(w)\, \exp\left(\frac{-Ew^2 N_s^2 R_{ww}(0)}{4\gamma}\right) \times \mathrm{sinc}\left(\frac{\sqrt{E}N_s R_{ww}(0)\left|h_o^u\right| w}{\pi}\right) dw. \quad (50)$$

The average BER is obtained by averaging $P_{e_{/h_o^u}}$ over $|h_o^u|$, and is given by $P_e = \int_0^\infty P_{e_{/h_o^u}} P_{|h_o^u|}(h)\, dh$.

VI. Numerical Results

A. Performance under AWGN Channels

In this section we present some numerical examples, aiming to verify the theoretical BER formulas derived. The derivations are independent of pulse shapes, but for simulation purposes the second derivative of the Gaussian pulse is assumed, i.e, $w(t) = \left[1 - 16\pi\left(t/T_m\right)^2\right]\exp\left[-8\pi\left(t/T_m\right)^2\right]$. The normalized autocorrelation of $w(t)$ is given by $R_{ww}(\tau) = \left[1 - 16\pi\left(t/T_m\right)^2 + \left(64\pi^2/3\right)\left(t/T_m\right)^4\right]\exp\left(-4\pi\left(t/T_m\right)^2\right)$ [9]. The following system parameters are assumed unless stated otherwise: $Nu = 25$, $N_h = 12$, and $\tau_m = 0.5ns$. Theoretical and simulation results of TH-PPM systems are compared in Fig. 4 for an orthogonal PPM system and in Fig. 5 for a non-orthogonal PPM system. Two different values; N_s = 4 an N_s = 8, are considered. Due to shorter chip duration, the upward turning of the curve towards the error floor occurs at lower SNR values in Fig. 5 compared to that in Fig. 4.

Fig. 6 and Fig. 7 compare the performances of TH-PAM for widely and closely spaced chips, respectively. Fig. 8 presents the DS-PAM system performance. In all the above cases the theoretical and simulation BER matches exactly. The simulations consider full asynchronous access and the results validate our theoretical derivations. The small deviations of the simulation curves from the theoretical curves are

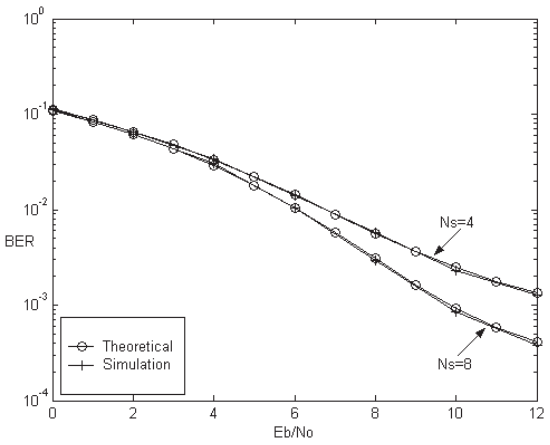

Fig. 5. Theoretical and simulation performance of TH-PPM compared for $N_s = 4$ and $N_s = 8$, with $T_c = 2ns$ and $\delta = 0.135ns$.

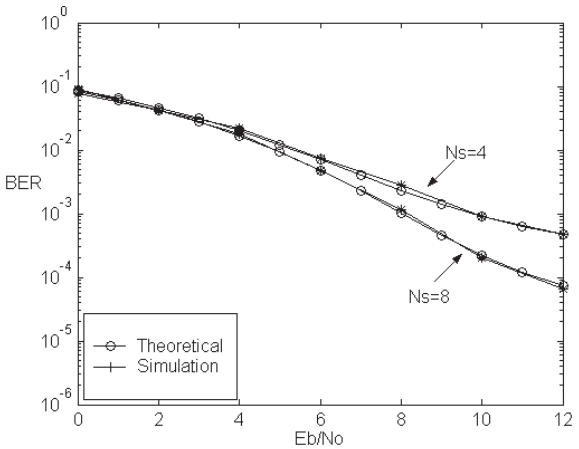

Fig. 7. Theoretical and simulation performance of TH-PAM compared for $N_s = 4$ and $N_s = 8$, with $T_c = 2ns$ (closely spaced chips).

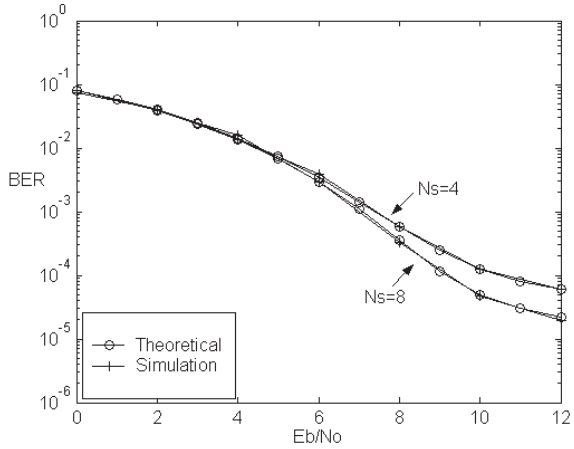

Fig. 6. Theoretical and simulation performance of TH-PAM compared for $N_s = 4$ and $N_s = 8$, with $T_c = 8ns$ (widely spaced chips).

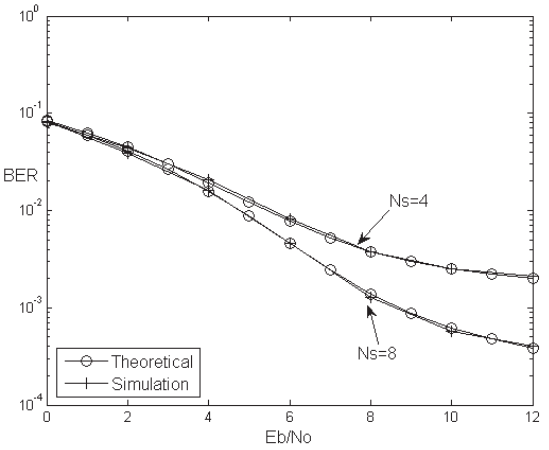

Fig. 8. Theoretical and simulation performance of DS-PAM compared for $N_s = 4$ and$N_s = 8$, with $T_c = 24ns$.

inevitable due to practical simulation inaccuracies which can be improved only by increasing the number of Monte-Carlo cycles.

In the theoretical evaluations, the BER is highly sensitive to the accuracy of the numerical integration at higher SNR values. The density of sampling points chosen and the truncation error involved in evaluating the infinite integrals in (23), (24), (25), (28), (31) (49) and (50) are the factors contributing to the error in numerical integration. Therefore large number of samples are needed and the truncation window should be larger at higher SNR values.

B. Performance in Fading Channels

To verify the equations for fading channels, the following parameters are used in conjunction with the channel model presented in Section II.D: $\sigma = 6$dB, $\mu_o^u = -1.3$, $\rho = 0.1408$ and $L = 10$. The theoretical performance curves presented for all the 3 systems agree well with the simulation curves. As explained in Section V.A, we used a combination of three different methods to accurately evaluate the CF over the possible ranges of values of μ. However, the segmentation of the range of μ does not have any clearly defined boundaries. These boundary values should be determined adaptively for each situation to minimize the estimation error, which also depend on the values of σ.

VII. Discussion and Conclusions

This paper presents the exact BER derivation of most common UWB systems. The MAI component contributed by a single interfering path is statistically modeled for a fully asynchronous multiple access system. It is also shown that the interference components contributed by individual template pulses are not independent. The proposed modeling of MAI fits exactly for the AWGN channel and it appropriately models the time variables associated in the MAI, even in channels with Poisson arrivals, with acceptable accuracy. This is verified by the simulation results. The extension of these derivations to the other schemes such as TH-OOK, DS-OOK and DS-PPM is quite straight forward using similar principles presented in this paper. Though this paper considers only binary modulation schemes, one can extend the method presented in this paper to derive exact BER equations for M-ary modulation schemes as well.

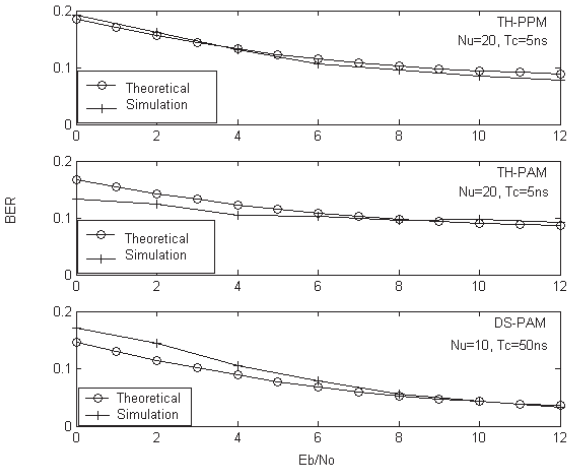

Fig. 9. Fading channel performance comparison of theoretical and simulation results.

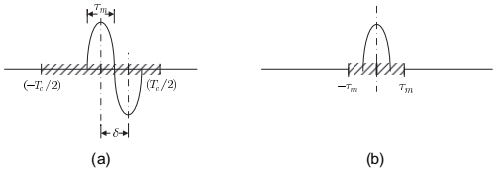

Fig. 10. (a) The first template pulse in the template wave form of PPM signal (enlarged). (b) The first template pulse in the template wave form of PAM signal (enlarged).

In the fading case, the evaluation of the CF of the total interference demands computational power due to the averaging of the conditional CF $\Phi_{I_l^u/I(\tau)}(w)$ over $I(\tau)$. But it should be noted that it is only necessary to numerically evaluate the CF of the total interference from the first path of a user. CFs of the other paths can be simply derived using (48). It should also be noted that, by appropriately modifying (48), different PDP can be adopted with fixed arrival times. Once the CF of the total interference from one user is available, estimation of BER for any number of users is straight forward. Therefore, the method proposed in this paper is useful in the performance analysis of practical UWB systems.

APPENDIX I

In this Appendix, the basic guidelines for deriving the probabilities are provided. Derivations are presented only for TH-PPM and TH-PAM. For DS-PAM these can be obtained in similar fashion. If the reader is interested in OOK modulation, the derivations for PAM can be used to infer the respective formulas since OOK can be considered as a varient of amplitude modulation.

DERIVATION OF THE PROBABILITIES FOR TH-PPM

Fig. 10a. is an enlarged version of a single template pulse in the desired user's template signal (here, we have selected the first template pulse without loss of generality). The range of τ is denoted by the shaded region. Due to the bit changeover, the template pulses in the desired user signal are divided into two sets, each having j and $N_s - j$ number of template pulses respectively. Since the position of bit changeover is a uniform random variable, each value that the variable j can take has an average probability $1/N_s$ over $j \in \{1, 2, .., N_s - 1\}$ and the two extremes $j = 0$ and $j = N_s$ have $1/2N_s$ probability. We will consider all the four possible dibit states separately.

Dibit state '00':

The related probabilities are denoted by$P_{00}(n_1)$. By considering the possible combinations of n_1 interfering pulses we obtain

$$P_{00}(n_1) = \frac{1}{4} C_{n_1}^{Ns} (1/N_h)^{n_1} (1 - 1/N_h)^{Ns - n_1}. \quad (51)$$

Dibit state '01':

In this case the interference contribution from the $(k-1)^{th}$ bit and the $(k)^{th}$ bit are, $n_1 R_{wb}(\tau)$ and $n_2 R_{wb}(\mu^-)$ respectively. By considering the available combinations for all the possible bit changeover positions we obtain

$$P_{01}(n_1, n_2) = \frac{1}{4} \sum_{j=n_1}^{(N_s - n_2)} P_j \, C_{n_1}^{j} (1/N_h)^{n_1} (1 - 1/N_h)^{(j - n_1)} \times C_{n_2}^{(N_s - j)} (1/N_h)^{n_2} (1 - 1/N_h)^{(N_s - j - n_2)}, \quad (52)$$

where $P_j = \begin{cases} 1/2N_s; & for\ j = 0, N_s \\ 1/N_s; & elsewhere \end{cases}$.

Dibit states '10' and '11':

The corresponding probabilities are defined by,$P_{10}(n_1, n_2)$ and$P_{11}(n_1)$. By noting the similarity with previous two cases we obtain, $P_{10}(n_1, n_2) = P_{01}(n_1, n_2)$, $P_{11}(n_1) = P_{00}(n_1)$. Therefore $P(n_1)$ in section III.B is given by $P(n_1) = P_{00}(n_1) + P_{11}(n_1)$.

APPENDIX II

DERIVATION OF THE PROBABILITIES FOR TH-PAM

The methodology is similar to that explained in Appendix I. Fig. 10b. is an enlarged version of a single template pulse in the desired user's template signal. Now, we consider the possible dibit combinations.

Dibit state '00':

$P_{00}(n_1) = 0$ for $n_1 < 0$, by considering the possible combinations$P_{00}(n_1)$ can be given by

$$P_{00}(n_1) = \tfrac{1}{4} C_{n_1}^{N_s} (1/N_h)^{n_1} (1 - 1/N_h)^{N_s - n_1}, \quad (53)$$

for $n_1 \in \{0, 1, ...Ns\}$.

Dibit state '01':

In this case the corresponding probability is given by

$$P_{01}(n_1) = \frac{1}{4} \sum_{j=|n_1|}^{N_s} P_j \sum_{r=0}^{\min(j-|n_1|,\, N_s - j)} C_{(|n_1|+r)}^{j} (1/N_h)^{|n_1|+r} \times (1 - 1/N_h)^{j - |n_1| - r} \, C_r^{N_s - j} (1/N_h)^{r} (1 - 1/N_h)^{N_s - j - r}, \quad (54)$$

Dibit states '10' and '11':

The probabilities for the dibit states '10' and '11' are respectively denoted by $P_{10}(n_1)$ and $P_{11}(n_1)$. By using the symmetry we get $P_{10}(n_1) = P_{01}(-n_1)$, for $n_1 \in \{-Ns.....Ns\}$, and $P_{11}(n_1) = P_{00}(-n_1)$, for $n_1 \in \{0, -1, ... - Ns\}$.

REFERENCES

[1] J. A. Ney da Silva and M. L. R. de Campos, "Performance Comparison of Binary and Quaternary UWB Modulation Schemes," in *Proc. IEEE GLOBECOM '03*, pp. 789-793, 1-5 Dec 2003.

[2] J. Zhang, T. D. Abhayapala, and R. A. Kennedy, "Performance of ultra-Wideband Correlator Receiver using Gaussian Monocycles," in *Proc. IEEE ICC '03*, pp. 2192-2196, May 2003.

[3] H. Liu, "Error performance of a pulse amplitude and position modulated ultra-wideband system over lognormal fading channels," *IEEE Commun. Lett*., vol. 7, pp. 531-533, Nov 2003.

[4] E. R. Bastidas-Puga, F. Ramirez-Mireles, and D. Munoz-Rodriguez, "Performance of UWB PPM in Residential Multi-Path Environments," in *Proc. IEEE VTC'03-Fall*, pp. 2307-2311, Oct. 2003 .

[5] J. D. Choi and W. E. Stark, "Performance of ultra-wideband communications with suboptimal receivers in multi-path channels," *IEEE Selected Areas Commun*., vol. 20, pp. 1754-1766, Dec 2002.

[6] D. Cassioli *et al.*, "Performance of Low-Complexity RAKE Reception in a Realistic UWB Channel," in *Proc. IEEE ICC'02*, pp. 763-767, 28 Apr.-2 May 2002.

[7] F. Ramirez-Mireles, "On the performance of ultra-wide-band signals in Gaussian noise and dense multi-path," *IEEE Trans. Vehic. Technol*., Vol. 50, pp. 244-249, Jan 2001.

[8] G. Durisi and S. Benedetto, "Performance Evaluation and Comparison of Different Modulation Schemes for UWB Multiaccess Systems," in *Proc. IEEE ICC'03*, pp. 2187-2191, May 2003.

[9] F. Ramirez-Mireles, "Performance of ultrawideband SSMA using time hopping and M-ary PPM," *IEEE J. Select. Areas Commun.*, vol. 19, pp. 1186-1196, June 2001.

[10] M. Z. Win and R. A. Scholtz, "Ultra-wide bandwidth time-hopping spread-spectrum impulse radio for wireless multiple-access communications," *IEEE Trans. Commun*., vol. 48, pp. 679-689, Apr. 2000.

[11] V. Venkatesan *et al.*, "Performance of an Optimally Spaced PPM Ultra-Wideband System with Direct Sequence Spreading for Multiple Access," in *Proc. IEEE VTC'03-Fall* , pp. 602-606 ,Oct. 2003.

[12] S. Niranjayan, A. Nallanathan, and B. Kannan, "Delay Tuning Based Transmit Diversity Scheme for TH-PPM UWB: Performance with RAKE Reception and Comparison with Multi RX Schemes", in *Proc. Joint UWBST and IWUWBS'04*, May 2004.

[13] G. Durisi and G. Romano, "On the validity of Gaussian Approximation to Characterize the Multiuser Capacity of UWB TH PPM," in *Proc. IEEE Conf. on Ultra Wideband Systems and Technologies 2002*, pp. 157-161, May 2002.

[14] A. R. Forouzan, M. Nasiri-Kenari, and J. A. Salehi, "Performance analysis of time-hopping spread-spectrum multiple-access systems: uncoded and coded schemes," *IEEE Trans. Wireless Commun.*, vol. 1, pp. 671-681, Oct. 2002.

[15] K. A. Hamdi and X. Gu, "On the validity of the gaussian Approximation for Performance Analysis of TH-CDMA/OOK Impulse Radio Networks," in *Proc. IEEE VTC'03-Spring*, pp. 2211-2215, Apr. 2003.

[16] B. Hu, and N.C Beaulieu, "Exact bit error rate analysis of TH-PPM UWB systems in the presence of multiple-access interference", *IEEE Comms. Lett*., vol. 7, pp. 572-574, Dec. 2003.

[17] M. Sabattini, E. Masry, and L. B. Milstein, "A Non-Gaussian Approach To The Performance Analysis of UWB TH-BPPM Systems," in *Proc EEE Conf. on Ultra Wideband Systems and Technologies*, Nov. 16-19, 2003, pp. 52 - 55.

[18] G. Durisi and S. Benedetto, "Performance evaluation of TH-PPM UWB systems in the presence of multiuser interference," *IEEE Commun. Lett*., vol. 7, pp. 224-226, May 2003.

[19] K. A. Hamdi and Xuanye Gu, "Bit Error Rate Analysis for TH-CDMA/PPM Impulse Radio Networks," in *Proc. IEEE WCNC'03*, pp. 167-172, 16-20 Mar. 2003.

[20] S. Niranjayan, A. Nallanathan and B. Kannan, "A New Analytical Method for Exact Bit Error Rate Computation of TH-PPM UWB Multiple Access Systems," in *Proc. IEEE PIMRC'04*, Sept. 2004.

[21] IEEE P802.15 Working Group for Wireless Personal Area Networks (WPANs), "Channel Modeling Sub-committee Report Final," Dec. 2002.

[22] A. F. Molisch, J. R Foerster, and M. Pendergrass, "Channel models for ultrawideband personal area networks," *IEEE Wireles Commun. Mag.,* Dec. 2003.

[23] N. C. Beaulieu, A. A. Abu-Dayya, and P. J. McLane, "Estimating the distribution of a sum of independent lognormal random variables," *IEEE Commun. Trans.*, pp. 2869-2873, Dec. 1995.

[24] N. C. Beaulieu, and Q. Xie, "An Optimal Lognormal Approximation to lognormal sum distributions," *IEEE Trans. Vechic. Technol.,* pp. 479 -489, April 2004.

[25] Roy B. Leipnik, "On lognormal random variables: I-the characteristic function," *J. Austral. Math. Soc.*, Ser. B 32(1991), pp. 327-347, 1991.

[26] M. S. Alouini, and A. J. Goldsmith, "A unified approach for calculating error rates of linearly modulated signals over generalized fading channels," *IEEE Commun. Trans.,*, pp. 1324-1334, Sept. 1999.

Somasundaram Niranjayan (S'03) received the B.Sc. degree with honors in electronic and telecommunication engineering from the University of Moratuwa, Sri-Lanka, in 2001 and the M.Eng. degree in electrical engineering from the National University of Singapore (NUS), Singapore, in 2004. He worked in the industry in electronics design from December 2002 to December 2003. Currently, he is working toward the Ph.D. degree at University of Alberta, Edmonton, Canada. His current research interests are ultra-wideband communication systems, communications in fading chanels, and wireless communications theory. He was a receipent of the NUS graduate scholarship.

Arumugam Nallanathan (S'97−M'00−SM'05) received the B.Sc. degree (with honors) from the University of Peradeniya, Peradeniya, Sri Lanka, in 1991, the C.P.G.S. degree from the University of Cambridge, Cambridge, U.K., in 1994, and the Ph.D. degree from the University of Hong Kong, Hong Kong, in 2000, all in electrical engineering. He is currently an Assistant Professor in the Department of Electrical and Computer Engineering, National University of Singapore, Singapore. His current research interests are high-speed data transmission over wireless links, orthogonal frequency division multiplexing, ultrawideband communications systems, and wireless communications theory.

Dr. Nallanathan currently serves as a Guest Editor for the *EURASIP Journal on Wireless Communications and Networking* Special issue on Ultra-Wideband Communication Systems-Technology and Applications. He also serves as an Associate Editor for the *IEEE Transactions on Wireless Communications*, the *IEEE Transactions on Vehicular Technology*, the *EURASIP Journal on Wireless Communications and Networking*, and the *Journal of Wireless Communications and Mobile Computing*.

Balakrishnan Kannan (S'97−M'01) received the B.Sc. and B.Eng. degrees from the University of Sydney, Australia, in 1994 and 1995 respectively, and the Ph.D.in electrical engineering from the University of Cambridge, United Kingdom, in 2001. He worked for Motorola, Singapore as an Electronic engineer for two years and for Institute for Infocomm Research, A*Star, Singapore as a Scientist for five years. He was also an Adjunct Assistant Professor at the National University of Singapore from 2001 until 2005. Currently, he is a Research Fellow at the University of New South Wales, Australia.

He was the secretary of the IEEE Singapore Section Communications Chapter in 2002 and 2003, and the treasurer for the 7th IEEE International Conference on Communication Systems (ICCS'02).

His research interests include array signal processing, space-time coding, adaptive signal processing, MIMO communication systems, ultra wide band impulse radio, and multi-rate multi-carrier communications systems. He has published around 40 papers in international conferences and journals.